

Robust photon blockade with hybrid molecular optomechanics

Jian Tang¹, Baijun Li², Bin Yin¹, Tian-Xiang Lu³, Ran Huang⁴✉, Franco Nori^{4,5} & Hui Jing^{1,6}✉

¹*Key Laboratory of Low-Dimensional Quantum Structures and Quantum Control of Ministry of Education, Hunan Normal University, Changsha 410081, China*

²*Research Center for Quantum Physics, Huzhou University, Huzhou 313000, China*

³*College of Physics and Electronic Information, Gannan Normal University, Ganzhou 341000, Jiangxi, China*

⁴*Quantum Information Physics Theory Research Team, Quantum Computing Center, RIKEN, Wako-shi, Saitama 351-0198, Japan*

⁵*Physics Department, The University of Michigan, Ann Arbor, Michigan 48109-1040, United States*

⁶*Institute for Quantum Science and Technology, College of Science, NUDT, Changsha 410073, P.R.China*

✉email: ran.huang@riken.jp; jinghui73@foxmail.com

Molecular cavity optomechanical systems, featuring ultrahigh vibrational frequencies and strong light-matter interactions, hold significant promise for advancing applications in quantum science and technology. Specifically, by introducing metallic nanoparticles into micro-cavities, hybrid molecular cavity optomechanical systems can further enhance optical quality factors and system tunabilities, which enables scalable and controllable quantum plat-

forms. In this study, we propose how to realize robust photon blockade, i.e., strong photon antibunching with arbitrary detuning conditions, by combining degenerate optical parametric amplification with a hybrid molecular cavity optomechanical system. More interesting, we find near-perfect optomechanical photon blockade at room temperature, which is robust against temperature and optical dissipation. In addition, our approach can release the strict condition of high temporal resolution by combining features of conventional and unconventional photon blockade. Our approach offers a feasible route to study intriguing quantum effects in hybrid molecular cavity optomechanical systems, and holds promise for applications in nonclassical state engineering, quantum sensing, and photonic precision measurements.

Introduction

Cavity optomechanical systems ^{1,2}, characterized by the interaction between optical fields and mechanical vibrations, offer a versatile platform for both fundamental research in physics and potential applications in high-precision sensing ³⁻⁹. Specifically, molecular vibrations, serving as nanoscale mechanical oscillators, exhibit exceptionally high resonant frequencies and strong optomechanical interactions with optical fields ¹⁰⁻¹². These features enable molecular cavity optomechanical systems to be remarkably resistant to temperature fluctuations and variations in system parameters. Therefore, molecular cavity optomechanical systems are ideal for applications such as heat transfer ¹³, optomechanically induced transparency ¹⁴, frequency up-conversion ¹⁵⁻¹⁷, metrology ¹⁸⁻²⁰, surface-enhanced Raman scattering ²¹, and molecular-protein analysis ²², as well as quantum heat engine ²³, and entanglement ²⁴.

Recent technological advances have enabled the integration of nanoparticles into high-quality microcavity platforms ²⁵. Hybrid molecular cavity optomechanical systems ^{26–28} have been proposed and studied using metallic nanoparticles combined with Fabry-Pérot resonators ²⁶, microdisk cavities ²⁷, or photonic crystals ²⁸. These hybrid platforms not only retain the high resonant frequencies and strong optomechanical interactions, but also exhibit higher optical quality factors ^{26–29}, exhibiting broad potential for various applications, such as microfilters and miniature spectrometers ³⁰. More importantly, the platforms enhance the scalability of molecular optomechanical systems, enabling flexible control via coupled cavity configurations.

Optical parametric amplification is a second-order nonlinear process, in which an optical signal is amplified by a pump via the generation of an idler field ³¹, and can be used to realize sources of biphotons ^{32–34}, squeezed light ^{35–38}, and highly nonclassical states of light ^{39,40}. Despite the inherently weak second-order nonlinearity, the large parametric gain can be achieved through strong pumping. Optical parametric amplification has been used to realize nonreciprocal optical transistor ⁴¹, phonon lasing ⁴², as well as entanglement between two atoms ⁴³, long-lived or entangled cat states ^{44,45}, tripartite quantum entanglement ⁴⁶, quantum sensing ^{47,48}, and photon blockade ^{49–51}. In the weak pump regime, the nonlinear process can be seen as a different excitation path ⁵⁰. This nonlinear process gives rise to destructive quantum interference between transition pathways, which is the fundamental mechanism of unconventional photon blockade ^{52–58}. Such nonlinear process induced photon blockade has been predicted in various platforms, including spinning cavity ⁵⁹, coupled cavities ⁶⁰, and cavity optomechanics ^{61,62}.

In this work, we propose how to realize robust photon blockade scheme by introducing a degenerate optical parametric amplifier within a hybrid molecular cavity optomechanical system. Specifically, by tuning the intensity and phase of the parametric gain, we can achieve strong photon antibunching under arbitrary detuning conditions. More interesting, we find near-perfect optomechanical photon blockade at room temperature, which is robust against temperature and optical dissipation. Furthermore, we find the oscillations in $g^{(2)}(\tau)$ can be eliminated, thus release the strict condition of high temporal resolution in experimental detection. Our approach offers a feasible route to achieve robust photon blockade using existing hybrid molecular molecular cavity optomechanical platforms and holds promise for applications in nonclassical state engineering, quantum sensing, and photonic precision measurements.

Model

We consider the following hybrid molecular cavity optomechanical system. A nanoparticle-on-mirror (NPoM) structure consists of a metallic nanoparticle deposited on a mirror, which forms a plasmonic nanocavity that resonates at frequency ω_c , as shown in the inset in Fig. 1a^{63–65}. A molecule is positioned in the nanoscale gap between the nanoparticle and the mirror, and is considered as a harmonic oscillator with a resonance frequency ω_b and a damping rate γ . This molecule couples to the plasmonic field via optomechanical interaction. By introducing an additional mirror, a Fabry-Pérot cavity is formed with resonance frequency ω_c , which contains a degenerate optical parametric amplifier. These components together form the hybrid molecular optomechanical system, as shown in Fig. 1a.

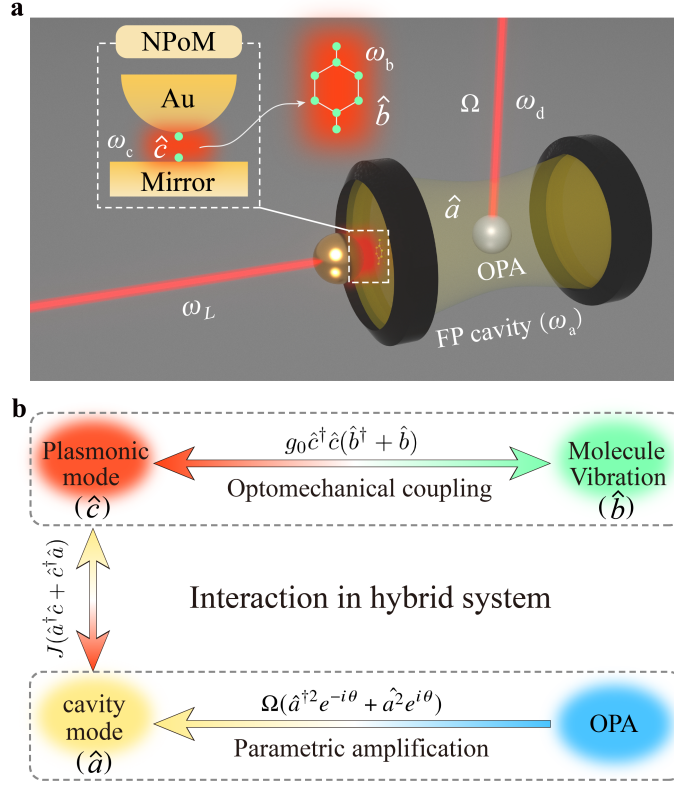


Fig. 1. Parametric amplification assistant hybrid molecule cavity optomechanical system.

a Schematic of the hybrid molecule cavity optomechanical system. A plasmonic nanocavity, formed by metallic nanoparticles and molecules deposited on a Fabry-Pérot (FP) cavity, is driven by an external laser of frequency ω_L . A degenerate optical parametric amplifier (OPA) inside the Fabry-Pérot cavity is driven by a laser of amplitude Ω and frequency ω_d . The inset shows the nanoparticle-on-mirror (NPoM) structure of the plasmonic nanocavity, where molecules is situated in the nanogap. **b** Schematic diagram of the equivalent mode-coupling model. The plasmonic nanocavity mode is coupled to the molecular vibrational (acoustic) mode via radiation pressure. This mode is also coupled to the Fabry-Pérot cavity mode (incorporating the parametric process) through evanescent fields interactions.

To achieve photon antibunching, we coherently drive the plasmonic nanocavity with a weak external field at frequency ω_L . Through the coupling between the two cavities (with strength J), this excitation populates the Fabry-Pérot cavity mode, which then interacts with the optical parametric amplifier driven by an external laser at frequency ω_p . The Hamiltonian for this three-mode system can be expressed as (assuming $\hbar = 1$):

$$\begin{aligned}\hat{H}_1 &= \omega_a \hat{a}^\dagger \hat{a} + \omega_c \hat{c}^\dagger \hat{c} + \omega_b \hat{b}^\dagger \hat{b} + \hat{H}_j + \hat{H}_d, \\ \hat{H}_j &= J(\hat{a}^\dagger \hat{c} + \hat{c}^\dagger \hat{a}) + g \hat{c}^\dagger \hat{c} (\hat{b}^\dagger + \hat{b}), \\ \hat{H}_d &= \xi (\hat{c} e^{i\omega_L t} + \text{H.c.}) + \Omega (\hat{a}^2 e^{i\theta} e^{i\omega_p t} + \text{H.c.}),\end{aligned}\tag{1}$$

where $\hat{a}(\hat{a}^\dagger)$, $\hat{c}(\hat{c}^\dagger)$, and $\hat{b}(\hat{b}^\dagger)$ represent the annihilation (creation) operators for the Fabry-Pérot cavity mode, the plasmonic nanocavity mode, and the molecular vibrational mode (phonons), respectively. Here, $g \hat{c}^\dagger \hat{c} (\hat{b}^\dagger + \hat{b})$ describes the optomechanical coupling interaction between the plasmonic nanocavity mode and the molecular vibrations. The coupling strength is given by $g = -\omega_c R_b \sqrt{\hbar/2m\omega_b}/(\epsilon_0 V_c)$ ^{11,12}, where R_b is the Raman polarizability, V_c is the effective volume of the plasmonic nanocavity mode, and ϵ_0 is the vacuum permittivity. In this work, we take as $R_b = 3 \times 10^{-10} \text{ } \epsilon_0^2 \text{ \AA}^4 \text{ amu}^{-1}$, and $V_c = 2.5 \text{ } \mu\text{m}^{-3}$ ^{11,12}, which yield $g/2\pi = 30 \text{ GHz}$. The optomechanical coupling coefficient g is estimated on the order between from $2\pi \times 10 \text{ GHz}$ to $2\pi \times 100 \text{ GHz}$, and from $\omega_b/2\pi \sim 6 \text{ THz}$ to 48 THz ¹⁰⁻¹². The driving amplitude ξ is expressed as $\xi = [\gamma_{\text{ex}} P_{\text{in}}/(\hbar\omega_L)]^{1/2}$, where P_{in} is the input driving power, and γ_{ex} is the external loss rate. The other parameters in our work are: $\omega_a/2\pi = \omega_c/2\pi = 460 \text{ THz}$, $\omega_b/2\pi = 30 \text{ THz}$, $Q_a = 10^6$, $Q_c = 46$, $\gamma/2\pi = 30 \text{ GHz}$, $J/2\pi = 3 \text{ THz}$. For the Fabry-Pérot cavities, the cavity quality factor $Q \sim 10^5 - 10^7$ ^{1,66}.

The final term in \hat{H}_d represents the coupling between the cavity field and the parametric amplifier with the parametric gain amplitude Ω and phase θ , which depends on the pump power and phase of the driving parametric amplifier, respectively⁶⁷. To clearly see the interaction relation in this hybrid molecular optomechanical system, we further show the schematic diagram of the equivalent mode-coupling mode in Fig. 1b.

By transforming the system into a rotating frame at the driving frequency ω_L and assuming the condition $\omega_p = 2\omega_L$, the Hamiltonian of system reads

$$\hat{H}_2 = \Delta_a \hat{a}^\dagger \hat{a} + \Delta_c \hat{c}^\dagger \hat{c} + \omega_m \hat{b}^\dagger \hat{b} + \hat{H}_j + \xi(\hat{c}^\dagger + \hat{c}) + \Omega(e^{-i\theta} \hat{a}^{\dagger 2} + e^{i\theta} \hat{a}^2), \quad (2)$$

where $\Delta_a = \omega_a - \omega_L$, $\Delta_c = \omega_c - \omega_L$. The quantum properties of light can be characterized by the second-order quantum correlation⁶⁸:

$$g^{(2)}(\tau) = \lim_{t \rightarrow \infty} \frac{\langle \hat{a}_1^\dagger(t) \hat{a}_1^\dagger(t + \tau) \hat{a}_1(t + \tau) \hat{a}_1(t) \rangle}{\langle \hat{a}_1^\dagger(t) \hat{a}_1(t) \rangle^2}, \quad (3)$$

which is usually measured by Hanbury Brown-Twiss interferometers^{69–73}. The condition $g^{(2)}(0) \ll 1$ indicates single-photon blockade with sub-Poissonian photon-number statistics^{69,74–76}. By introducing the density matrix of the cavity field $\rho(t)$ and Lindblad superoperator $D[O](\rho) = [O, \rho] = 2O\rho O^\dagger - OO^\dagger\rho - \rho O^\dagger O$, (where $O = a, b, c$), this $g^{(2)}(\tau)$ [or $g^{(2)}(0)$] can be calculated by numerically solving the Lindblad master equation of this system^{77,78}:

$$\begin{aligned} L = & -i[H_2, \rho] + \frac{\kappa_a(n_a + 1)}{2} D[\hat{a}] + \frac{\kappa_a n_a}{2} D[\hat{a}^\dagger] \\ & + \frac{\kappa_c(n_c + 1)}{2} D[\hat{c}] + \frac{\kappa_c n_c}{2} D[\hat{c}^\dagger] \\ & + \frac{\gamma(n_b + 1)}{2} D[b] + \frac{\gamma n_b}{2} D[b^\dagger], \end{aligned} \quad (4)$$

where $n_{b(a,c)} = [\exp(\hbar\omega_{b(a,c)}/(k_b T)) - 1]^{-1}$ is the mean thermal phonon (photon) number of the mechanical (optical) mode at temperature T , with the Boltzmann constant k_b . The decay rate of the cavity (plasmonic) mode is given by $\kappa_a = \omega_a/Q_a$ ($\kappa_c = \omega_c/Q_c$).

Results

To diagonalize the Hamiltonian, we introduce the following unitary operator $\hat{U}(\beta_0) = e^{\beta_0 \hat{c}^\dagger \hat{c} (\hat{b}^\dagger - \hat{b})}$, where $\beta_0 = -g_0/\omega_m$. Using the fact that $g_0 \ll \omega_m$, we can safely neglect small exponential terms, allowing the mechanical mode of molecular vibrations to decouple from the plasmonic nanocavity mode. It is easy to make a unitary transformation on the Hamiltonian of the Molecular cavity optomechanical system:

$$\begin{aligned} \hat{H}_3 = \hat{U} \hat{H}_2 \hat{U}^\dagger &= \Delta \hat{a}^\dagger \hat{a} + \Delta \hat{c}^\dagger \hat{c} + J \left(\hat{a}^\dagger \hat{c} + \hat{a} \hat{c}^\dagger \right) - G \left(\hat{c}^\dagger \hat{c} \right)^2 \\ &+ \xi \left(\hat{c}^\dagger + \hat{c} \right) + \Omega \left(\hat{a}^{\dagger 2} e^{-i\theta} + \hat{a}^2 e^{i\theta} \right), \end{aligned} \quad (5)$$

where $G = \frac{g_0^2}{\omega_m}$. Here, we wrote in a frame where the pump and signal modes phase space rotate at frequency ω_L . In accordance with the quantum trajectory method ⁷⁹, the decay of optical can be included in the effective Hamiltonian.

$$\hat{H}_{\text{eff}} = \hat{H}_3 - \frac{i\kappa_a}{2} \hat{a}^\dagger \hat{a} - \frac{i\kappa_c}{2} \hat{c}^\dagger \hat{c}. \quad (6)$$

Under the weak-driving condition ($\xi \ll \gamma$), the Hilbert space can be restricted to $N = M + N = 3$.

The state of this system can be expressed as

$$|\psi(t)\rangle = \sum_{N=0}^3 \sum_{m=0}^N C_{m,N-m} |m, N-m\rangle, \quad (7)$$

with probability amplitudes $C_{m,N-m}$, which can be obtained by solving the Schrödinger equation

$$i|\dot{\psi}(t)\rangle = \hat{H}_{\text{eff}}|\psi(t)\rangle. \quad (8)$$

Based on the effective Hamiltonian \hat{H}_{eff} and the wave function, We can obtain the steady-state equations of the probability amplitudes. For $C_{00}(t)$, we have $i\dot{C}_{00}(t) = 0$, while the other amplitudes fulfil the following equations:

$$\begin{aligned} 0 &= \Delta_1 C_{1,0} + J C_{0,1} + \xi C_{1,1}, \\ 0 &= \Delta_2 C_{0,1} + J C_{1,0} + \xi C_{0,0} + \sqrt{2}\xi C_{0,2}, \\ 0 &= 2\Delta_1 C_{2,0} + \sqrt{2}J C_{1,1} + \sqrt{2}\Omega e^{i\theta} C_{0,0}, \\ 0 &= (\Delta_1 + \Delta_2) C_{1,1} + \sqrt{2}J C_{0,2} + \sqrt{2}J C_{2,0} + \xi C_{1,0}, \\ 0 &= 2\Delta_2 C_{0,2} + \sqrt{2}J C_{1,1} + \sqrt{2}\xi C_{0,1}. \end{aligned} \quad (9)$$

Here, we have $\Delta_1 = \Delta_c - \frac{i\kappa_a}{2}$, $\Delta_2 = \Delta_c - G - \frac{i\kappa_c}{2}$.

We obtain the following solutions by considering the initial condition $C_{00}(0) = 1$:

$$\begin{aligned} C_{10} &= \frac{-\xi\Delta}{\eta_1}, \\ C_{20} &= \frac{\sqrt{2}\xi^2 J^2 (\Delta_1 + \Delta_2 - G) - \sqrt{2}\Omega e^{i\theta} \eta_1 \eta_2}{\eta_1 \eta_3}, \end{aligned} \quad (10)$$

where $\eta_1 = \Delta_1 \Delta_2 - J^2$, $\eta_2 = \eta_1 + \Delta_2^2 - (\Delta_1 + \Delta_2)G$, $\eta_3 = 2\Delta_1 \eta_2 - 2J^2(\Delta_2 - G)$. Since $|C_{10}|^2 \gg |C_{20}|^2$ and $|C_{10}|^2 \gg |C_{11}|^2$, the second-order correlation function can be written as

$$g^{(2)}(0) = \frac{2|C_{20}|^2}{(|C_{10}|^2 + 2|C_{20}|^2 + |C_{11}|^2)^2} \approx \frac{2|C_{20}|^2}{|C_{10}|^4}. \quad (11)$$

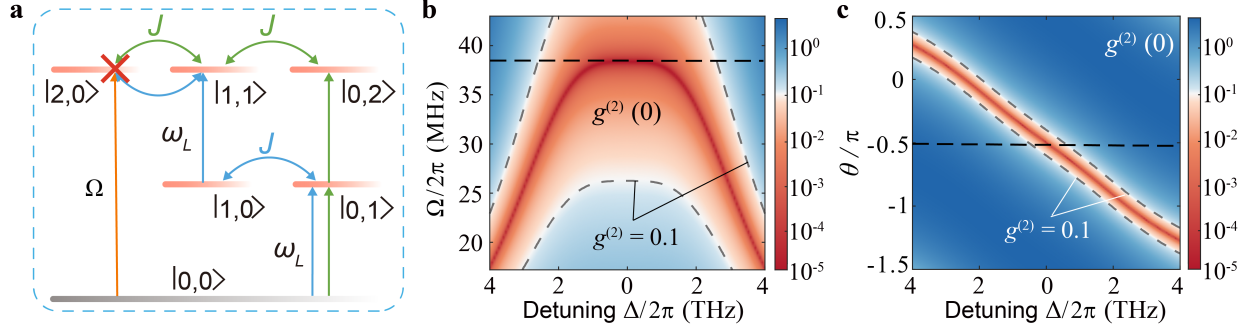


Fig. 2. The mechanism and optimal parametric gain conditions of molecular optomechanical photon blockade. **a** The destructive interference of the three transition from state $|0,0\rangle$ to state $|2,0\rangle$ (red, blue, green arrows) prevents two-photon occupation, enabling the unconventional photon blockade effect. **b** Second-order correlation $g^{(2)}(0)$ as a function versus detuning Δ and parametric gain amplitude Ω . **c** Quantum correlation $g^{(2)}(0)$ as a function versus of detuning Δ and parametric gain phase θ . Here, $P_{\text{in}} = 0.1 \text{ nW}$, $T = 0\text{K}$. The other parameters are given in the main text.

The photon blockade can occur with $P_{20} = 0$ ^{52,55,57}, which can be attributed to the destructive interference among three transition paths, as illustrated in Fig. 2a: $|0,0\rangle \xrightarrow{\Omega} |2,0\rangle$, $|0,0\rangle \xrightarrow{\omega_L} |0,1\rangle \xrightarrow{\omega_L} |0,2\rangle \xrightarrow{\sqrt{2}J} |1,1\rangle \xrightarrow{\sqrt{2}J} |2,0\rangle$, and $|1,0\rangle \xrightarrow{J} |0,1\rangle \xrightarrow{\omega_L} |1,1\rangle \xrightarrow{\sqrt{2}J} |2,0\rangle$. Thus, the optimal parametric gain satisfies

$$\begin{aligned}\Omega_{\text{opt}} &= \frac{|\xi^2 J^2 (\Delta_1 + \Delta_2 - G)|}{|\eta_1 \eta_2|}, \\ \theta_{\text{opt}} &= \arg[\xi^2 J^2 (\Delta_1 + \Delta_2 - G)] - \arg(\eta_1 \eta_2).\end{aligned}\quad (12)$$

We plot the second-order correlation function $g^{(2)}(0)$ as a function of detuning and parametric gain amplitude (or phase), as shown in Figs. 2b, c, where the curves represent $g^{(2)}(0) = 0.1$. The

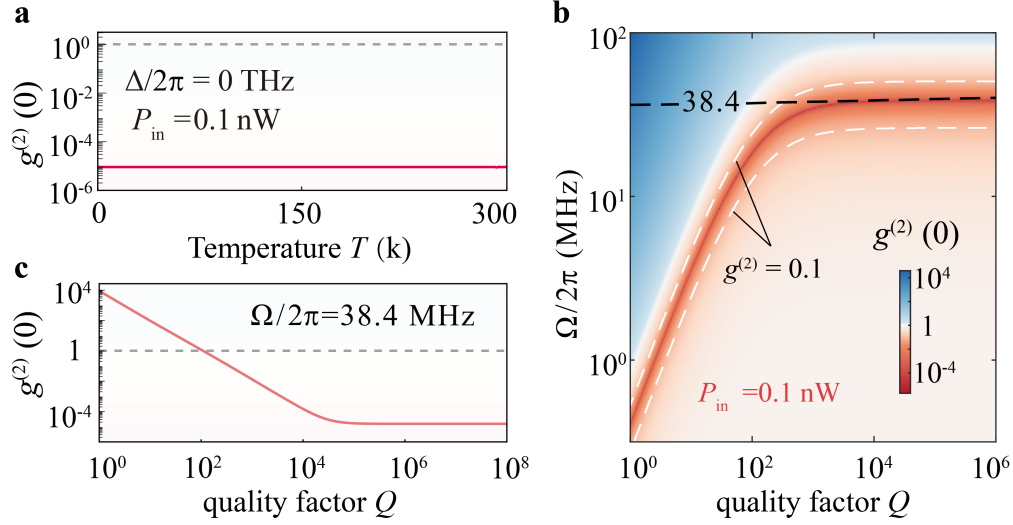


Fig. 3. Robustness of the molecular optomechanical photon blockade against varying temperature and cavity quality factor. **a** The second-order correlation function $g^{(2)}(0)$ versus T at driving power $P_{\text{in}} = 0.1$ nW and $\Delta/2\pi = 0$ THz, showing that $g^{(2)}(0) \ll 1$ under room-temperature conditions, thereby demonstrating robust photon blockade in the presence of thermal effects. **b** Influence of the cavity quality factor Q on unconventional photon blockade at an input power of $P_{\text{in}} = 0.1$ nW. Across a broad range of Q values, perfect unconventional photon blockade can be achieved by properly tuning the Ω , and the optimal Ω is consistent in the high- Q regime. **c** For $\Omega/2\pi = 38.4$ MHz, $g^{(2)}(0)$ remains effectively insensitive to Q for $Q > 10^5$, demonstrating the minimal impact of the cavity quality factor on unconventional photon blockade under these conditions. The other parameters are the same as those in Fig. 2.

robust photon blockade can be achieved across a wide range of detunings by appropriately tuning the parametric gain amplitude and phase. As the detuning $\Delta/2\pi$ decreases, the gain amplitude Ω must be increased to maintain the optimal blockade conditions.

Our results show that photon blockade in this system exhibits remarkable robustness to temperature variations. As temperature increases, the thermal occupations of phonons ($n_b = [\exp(\hbar\omega_b/(k_bT)) - 1]^{-1}$) rise, typically weakening photon blockade in conventional optomechanical systems. In contrast, the molecular optomechanical system features an acoustic mode frequency of molecular vibrations that is sufficiently high ($\omega_b/2\pi = 30$ THz) to keep phonon occupation comparatively low ($n_b \approx 0.8$), even at room temperature. While the photon thermal occupation remains negligible, allowing the photon blockade effect to persist essentially undisturbed, as illustrated in Fig. 3 a.

We further find that single-photon blockade is robust against the quality factor of the coupled Fabry-Pérot cavity. As illustrated in Fig. 3b, strong antibunching ($g_2 \ll 1$) is observed at $Q = 1$ by tuning the parametric strength, indicating that single-photon blockade can be achieved even in low- Q cavities. For high- Q cavities, the optimal parametric strength for single-photon blockade stabilizes and does not vary significantly. Hence, as shown in Fig. 3c, once the Fabry-Pérot cavity quality factor Q exceeds 10^5 , the parametric gain for unconventional photon blockade remain nearly unchanged, eliminating the need for stringent cavity design or measurement to achieve robust single-photon blockade.

Finally, we find that our approach can release the strict condition of high temporal resolution in photon correlation measurements. As the detuning Δ decreases, the optimal parametric gain amplitude Ω required to achieve photon blockade increases accordingly, while the time-dependent second-order correlation function $g^{(2)}(\tau)$ gradually becomes oscillation-free. Specifically, for

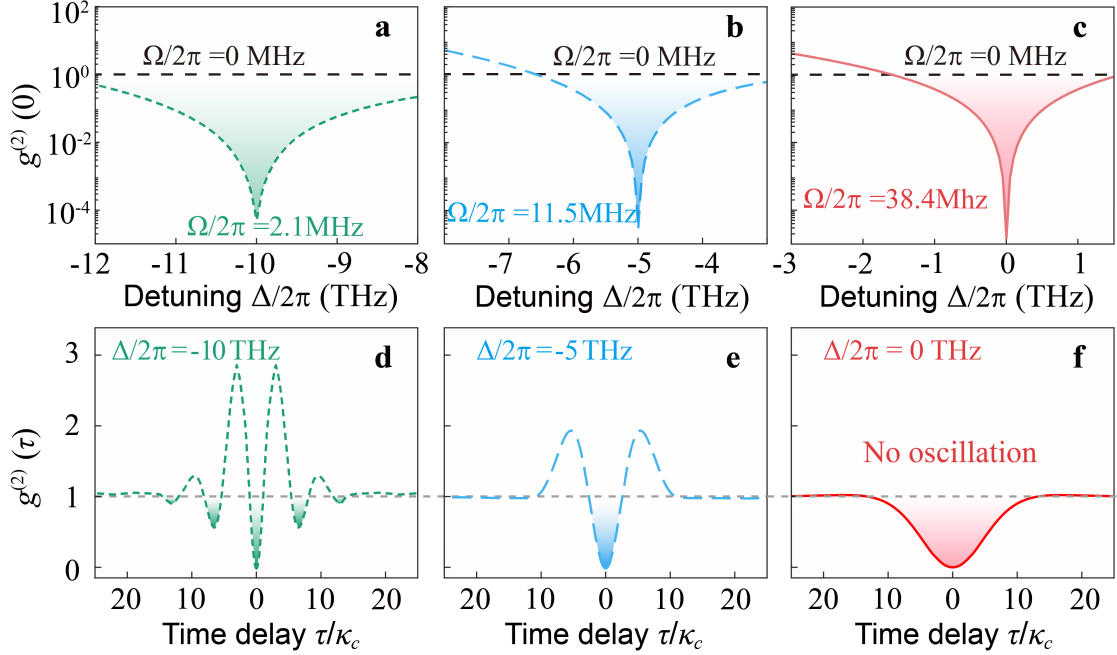


Fig. 4. Robust and oscillation-free photon blockade over time. For **a** $\Delta/2\pi = -10$ THz, **b** $\Delta/2\pi = -5$ THz and **c** $\Delta/2\pi = 0$ THz, the optimal parametric gain amplitude for realizing robust photon blockade is $\Omega/2\pi = 2.1$ MHz, $\Omega/2\pi = 11.5$ MHz and $\Omega/2\pi = 38.4$ MHz, respectively. **d**, **e**, **f** The evolution of the second-order correlation function $g^{(2)}(\tau)$ with respect to the time delay τ/γ , showing no oscillations at $\Delta = 0$, thereby indicating that high temporal resolution is not needed to observe photon blockade in this regime. Here, $P_{\text{in}} = 0.1$ nW, and the other parameters are the same as those in Fig. 2.

$\Delta/2\pi = -10$ THz and -5 THz, robust photon blockade is obtained at $\Omega/2\pi = 2.1$ MHz and 11.5 MHz, respectively [Figs. 4a, b]. In these cases, although $g^{(2)}(0)$ is significantly suppressed, oscillations still appear in $g^{(2)}(\tau)$ during evolution [Figs. 4d, e]. Remarkably, at zero detuning ($\Delta/2\pi = 0$ THz), the minimum of $g^{(2)}(0)$ is achieved at $\Omega/2\pi = 38.4$ MHz [Figs. 4c]. And the system exhibits features of both conventional and unconventional photon blockade: $g^{(2)}(0)$ remains

well below unity while the temporal oscillations in $g^{(2)}(\tau)$ are completely eliminated [Figs. 4f]. As a result, the antibunching persists over a prolonged duration of nearly $10\kappa_c$ ($\kappa_c/2\pi = 10$ THz), indicating that photon blockade can be observed reliably and without the need for high temporal resolution in detection.

DISCUSSION

In summary, we have proposed how to realize a robust photon blockade scheme based on a hybrid molecular cavity optomechanical system introducing a degenerate optical parametric amplifier. By tuning the parametric gain amplitude and phase, strong photon antibunching is achieved across a wide range of detuning. Owing to the high-frequency molecular vibrations and enhanced optomechanical coupling, the system exhibits remarkable resilience against variations in temperature and optical dissipation, maintaining nonclassical photon statistics even under room-temperature conditions. Furthermore, the system exhibits both conventional and unconventional photon blockade characteristics, i.e., $g^{(2)}(0)$ remains well below unity while the temporal oscillations in $g^{(2)}(\tau)$ are completely eliminated. This allows photon blockade to be observed without the need for high temporal resolution, improving experimental feasibility.

This work highlights the unique advantages of hybrid molecular cavity optomechanical systems, which combine nanoscale mechanical degrees of freedom with high optical quality factors and strong light–matter interactions. These features make such systems promising platforms for realizing a range of quantum effects beyond photon blockade, including light-motion entangle-

ment ^{80–83}, optomechanical cat states ^{84–86}, photon bundles ^{87–90}, and thermally robust squeezed or correlated states ^{37,38}. Moreover, the intrinsic resilience of system to environmental decoherence makes it particularly attractive for applications in quantum sensing and precision measurement under ambient conditions. Our findings offer a foundation for exploring broader functionalities of hybrid optomechanical architectures in integrated quantum photonics.

Data Availability

All relevant data that support the figures within this paper and other findings of this study are available from the corresponding authors upon reasonable request.

Code Availability

All relevant code support the figures within this paper and other findings of this study are available from the corresponding authors upon reasonable request.

Funding H.J. is supported by the National Key R&D Program (Grant No. 2024YFE0102400), the National Natural Science Foundation of China (Grants No. 11935006 and No. 12421005), the Hunan Major Sci-Tech Program (Grant No. 2023ZJ1010). R.H. is supported by the RIKEN Special Postdoctoral Researchers (SPDR) program. X.-W.X. is supported by the Innovation Program for Quantum Science and Technology (Grant No. 2024ZD0301000). T.-X.L. is supported by the NSFC (Grant No. 12565001, 12205054) and the Natural Science Foundation of Jiangxi Province (No. 20252BAC200163). F.N. is supported by the Japan Science and Technology Agency (JST) [via the CREST Quantum Frontiers program

Grant No. JPMJCR24I2, the Quantum Leap Flagship Program (Q-LEAP), and the Moonshot R&D Grant No. JPMJMS20611], the Office of Naval Research (ONR) Global (via Grant No. N62909-23-1-2074), and the National Science Foundation (NSF) NQVL: QSDT Award No. 2435166.

Acknowledgements The authors thank Xun-Wei Xu for helpful discussions.

Author Contributions H.J. designed and supervised the project. R.H. advised on the interpretation of the results. J.T. performed the research and wrote the manuscript. B.-J.L discussed the results. B.Y. prepared figure 1. F.N. and T.-X.L revised the manuscript. All authors discussed the results and reviewed the manuscript.

Competing Interests The authors declare that they have no competing financial interests.

Correspondence and requests for materials should be addressed to H. J and R.H.

References

1. Aspelmeyer, M, Kippenberg, T J and Marquardt, F. Cavity optomechanics. *Rev. Mod. Phys.* **86**, 1391 (2014).
2. Metcalfe, M. Applications of cavity optomechanics. *Appl. Phys. Rev.* **1**, 031105 (2014).
3. Aspelmeyer, M, Meystre, P and Schwab, K. Quantum optomechanics. *Phys. Today* **65**, 29 (2012).
4. Kippenberg, T J and Vahala, K J. Cavity optomechanics: back-action at the mesoscale. *Science* **321**, 1172 (2008).

5. Brennecke, F, Ritter, S and Donner, T *et al.* Cavity optomechanics with a Bose-Einstein condensate. *Science* **322**, 235 (2008).
6. Pirkkalainen, J-M, Cho, S and Massel, F *et al.* Cavity optomechanics mediated by a quantum two-level system. *Nat. Commun.* **6**, 6981 (2015).
7. Li, B-B, Ou, L and Lei, Y *et al.* Cavity optomechanical sensing. *Nanophotonics* **10**, 2799 (2021).
8. Zhu, G-L, Hu, C-S and Wu, Y *et al.* Cavity optomechanical chaos. *Fundam. Res.* **3**, 63 (2023).
9. Xu, J, Mao, Y and Li, Z *et al.* Single-cavity loss-enabled nanometrology. *Nat. Nanotechnol.* (2024).
10. Benz, F, Schmidt, M K and Dreismann, A *et al.* Single-molecule optomechanics in "picocavities". *Science* **354**, 726 (2016).
11. Roelli, P, Galland, C and Piro, N *et al.* Molecular cavity optomechanics as a theory of plasmon-enhanced Raman scattering. *Nat. Nanotechnol.* **11**, 164 (2016).
12. Esteban, R, Baumberg, J J and Aizpurua, J. Molecular optomechanics approach to surface-enhanced Raman scattering. *Acc. Chem. Res.* **55**, 1889–1899 (2022).
13. Ashrafi, S M, Malekfar, R and Bahrapour, A R *et al.* Optomechanical heat transfer between molecules in a nanoplasmonic cavity. *Phys. Rev. A* **100**, 013826 (2019).

14. Yin, B, Wang, J and Peng, M-Y *et al.* Molecular optomechanically induced transparency. *Phys. Rev. A* **111**, 043507 (2025).
15. Zou, F, Du, L and Li, Y *et al.* Amplifying frequency up-converted infrared signals with a molecular optomechanical cavity. *Phys. Rev. Lett.* **132**, 153602 (2024).
16. Chen, W, Roelli, P and Hu, H *et al.* Continuous-wave frequency upconversion with a molecular optomechanical nanocavity. *Science* **374**, 1264 (2021).
17. Xomalis, A, Zheng, X and Chikkaraddy, R *et al.* Detecting mid-infrared light by molecular frequency upconversion in dual-wavelength nanoantennas. *Science* **374**, 1268 (2021).
18. Liu, J and Zhu, K-D. Room temperature optical mass sensor with an artificial molecular structure based on surface plasmon optomechanics. *Photon. Res.* **6**, 867 (2018).
19. Liu, J and Zhu, K-D. Coupled quantum molecular cavity optomechanics with surface plasmon enhancement. *Photon. Res.* **5**, 450 (2018).
20. Tabatabaei, M, Najarianiini, M and Davieau, K *et al.* Tunable 3D plasmonic cavity nanosensors for surface-enhanced Raman spectroscopy with sub-femtomolar limit of detection. *ACS Photon.* **2**, 752 (2015).
21. Zhang, Y, Aizpurua, J and Esteban, R. Optomechanical collective effects in surface-enhanced Raman scattering from many molecules. *ACS Photon.* **7**, 1676 (2020).

22. Sadhanasatish, T, Augustin, K and Windgasse, L *et al.* A molecular optomechanics approach reveals functional relevance of force transduction across talin and desmoplakin. *Sci. Adv.* **9**, eadg3347 (2023).
23. Zhu, B, Meystre, P and Zhang, W *et al.* Autonomous quantum heat engine enabled by molecular optomechanics and hysteresis switching. *arXiv*.
24. Huang, J, Lei, D and Agarwal, G S *et al.* Collective quantum entanglement in molecular cavity optomechanics. *Phys. Rev. B* **110**, 184306 (2024).
25. Zhang, T, Wang, Y and Hua, Q. Plasmonic-photonic crystal hybrid devices for optical characterization. *J. Phys. D: Appl. Phys.* **57**, 363001 (2024).
26. Shlesinger, I, Vandersmissen, J and Oksenberg, E *et al.* Hybrid cavity-antenna architecture for strong and tunable sideband-selective molecular Raman scattering enhancement. *Sci. Adv.* **9**, eadj4637 (2023).
27. Shlesinger, I, Cognée, K G and Verhagen, E *et al.* Integrated molecular optomechanics with hybrid dielectric–metallic resonators. *ACS Photon.* **8**, 3506–3516 (2021).
28. Dezfouli, M K, Gordon, R and Hughes, S. Molecular optomechanics in the anharmonic cavity-QED regime using hybrid metal–dielectric cavity modes. *ACS Photon.* **6**, 1400–1408 (2019).
29. Barreda, A I, Zapata-Herrera, M and Palstra, I M *et al.* Hybrid photonic-plasmonic cavities based on the nanoparticle-on-a-mirror configuration. *Photon. Res.* **9**, 2398–2419 (2021).

30. Zhang, Y, Zhang, S and Wu, H *et al.*. Miniature computational spectrometer with a plasmonic nanoparticles-in-cavity microfilter array. *Nat. Commun.* **15**, 3807 (2024).
31. Shen, Y R. *Principles of Nonlinear Optics*. Wiley-Interscience, NY, USA (1984).
32. U'Ren, A B, Silberhorn, C and Erdmann, R *et al.*. Generation of pure-state single-photon wavepackets by conditional preparation based on spontaneous parametric downconversion. *arXiv:quant-ph/0611019* (2006).
33. Mosley, P J, Lundeen, J S and Smith, B J *et al.*. Heralded generation of ultrafast single photons in pure quantum states. *Phys. Rev. Lett.* **100**, 133601 (2008).
34. Harris, S E. Chirp and compress: Toward single-cycle biphotons. *Phys. Rev. Lett.* **98**, 063602 (2007).
35. Crouch, D D. Broadband squeezing via degenerate parametric amplification. *Phys. Rev. A* **38**, 508–511 (1988).
36. Kashiwazaki, T, Takanashi, N and Yamashima, T *et al.*. Continuous-wave 6-db-squeezed light with 2.5-thz-bandwidth from single-mode PPLN waveguide. *APL Photon.* **5**, 036104 (2020).
37. Qin, W, Miranowicz, A and Nori, F. Beating the 3 dB limit for intracavity squeezing and its application to nondemolition qubit readout. *Phys. Rev. Lett.* **129**, 123602 (2022).
38. Kawasaki, A, Ide, R and Brunel, H *et al.*. Broadband generation and tomography of non-Gaussian states for ultra-fast optical quantum processors. *Nat. Commun.* **15**, 9075 (2024).

39. Yan, Z-H, Qin, J-L and Qin, Z-Z *et al.*. Generation of non-classical states of light and their application in deterministic quantum teleportation. *Fundam. Res.* **1**, 43–49 (2021).
40. Hou, F-Y, Yu, L and Jia, X-J *et al.*. Experimental generation of optical non-classical states of light with 1.34 μm wavelength. *Eur. Phys. J. D* **62**, 433–437 (2011).
41. Tang, L, Tang, J and Chen, M *et al.*. Quantum squeezing induced optical nonreciprocity. *Phys. Rev. Lett.* **128**, 083604 (2022).
42. Lu, T-X, Wang, Y and Xia, K *et al.*. Quantum squeezing induced nonreciprocal phonon laser. *Sci. China Phys. Mech. Astron.* **67**, 260312 (2024).
43. Qin, W, Miranowicz, A and Li, P-B *et al.*. Exponentially enhanced light-matter interaction, cooperativities, and steady-state entanglement using parametric amplification. *Phys. Rev. Lett.* **120**, 093601 (2018).
44. Qin, W, Miranowicz, A and Jing, H *et al.*. Generating long-lived macroscopically distinct superposition states in atomic ensembles. *Phys. Rev. Lett.* **127**, 093602 (2021).
45. Chen, Y-H, Qin, W and Wang, X *et al.*. Shortcuts to adiabaticity for the quantum Rabi model: Efficient generation of giant entangled cat states via parametric amplification. *Phys. Rev. Lett.* **126**, 023602 (2021).
46. Jiao, Y-F, Zuo, Y-L and Wang, Y *et al.*. Tripartite quantum entanglement with squeezed optomechanics. *Laser Photon. Rev.* **18**, 2301154 (2024).

47. Wang, J, Zhang, Q and Jing, H. Quantum weak torque sensing with squeezed optomechanics. *Phys. Rev. A* **110**, 033505 (2024).
48. Zhang, S-D, Wang, J and Zhang, Q *et al.* Squeezing-enhanced quantum sensing with quadratic optomechanics. *Opt. Quantum* **2**, 222–229 (2024).
49. Lü, X-Y, Wu, Y and Johansson, J R *et al.* Squeezed optomechanics with phase-matched amplification and dissipation. *Phys. Rev. Lett.* **114**, 093602 (2015).
50. Wang, D-Y, Yan, L-L and Su, S-L *et al.* Squeezing-induced nonreciprocal photon blockade in an optomechanical microresonator. *Opt. Express* **31**, 22343–22357 (2023).
51. Shen, C-P, Chen, J-Q and Pan, X-F *et al.* Tunable nonreciprocal photon correlations induced by directional quantum squeezing. *Phys. Rev. A* **108**, 023716 (2023).
52. Liew, T C H and Savona, V. Single photons from coupled quantum modes. *Phys. Rev. Lett.* **104**, 183601 (2010).
53. Snijders, H J, Frey, J A and Norman, J *et al.* Observation of the unconventional photon blockade. *Phys. Rev. Lett.* **121**, 043601 (2018).
54. Vaneph, C, Morvan, A and Aiello, G *et al.* Observation of the unconventional photon blockade in the microwave domain. *Phys. Rev. Lett.* **121**, 043602 (2018).
55. Flayac, H and Savona, V. Unconventional photon blockade. *Phys. Rev. A* **96**, 053810 (2017).
56. Jabri, H and Eleuch, H. Enhanced unconventional photon-blockade effect in one- and two-qubit cavities interacting with nonclassical light. *Phys. Rev. A* **106**, 023704 (2022).

57. Bamba, M, Imamoğlu, A and Carusotto, I. Origin of strong photon antibunching in weakly nonlinear photonic molecules. *Phys. Rev. A* **83**, 021802 (2011).
58. Li, B, Huang, R and Xu, X *et al.* Nonreciprocal unconventional photon blockade in a spinning optomechanical system. *Photonics Res.* **7**, 630 (2019).
59. Shen, H-Z, Wang, Q and Wang, J. Nonreciprocal unconventional photon blockade in a driven dissipative cavity with parametric amplification. *Phys. Rev. A* **101**, 013826 (2020).
60. Gou, C and Hu, X. Simultaneous nonreciprocal photon blockade in two coupled spinning resonators via sagnac-fizeau shift and parametric amplification. *Phys. Rev. A* **108**, 043723 (2023).
61. Wang, D-Y, Bai, C-H and Han, X *et al.* Enhanced photon blockade in an optomechanical system with parametric amplification. *Opt. Lett.* **45**, 2604–2607 (2020).
62. Xie, H, He, L-W and Shang, X. Photon blockade in cavity optomechanics via parametric amplification. *Adv. Quantum Technol.* **7**, 2400065 (2024).
63. Peng, W, Zhou, J-W and Li, M-L *et al.* Construction of nanoparticle-on-mirror nanocavities and their applications in plasmon-enhanced spectroscopy. *Chem. Sci.* **15**, 2697–2711 (2024).
64. Hu, H, Xu, Y and Hu, Z *et al.* Nanoparticle-on-mirror pairs: building blocks for remote spectroscopies. *Nanophotonics* **11**, 5153–5163 (2022).
65. Li, Y, Chen, W and He, X *et al.* Boosting light matter interactions in plasmonic nanogaps. *Adv. Mater.* **36**, 2405186 (2024).

66. Galinskiy, I, Tsaturyan, Y and Parniak, M. Phonon counting thermometry of an ultracoherent membrane resonator near its motional ground state. *Optica* **7**, 718–725 (2020).
67. Qin, W, Miranowicz, A, and Li, P-B *et al.* Exponentially Enhanced Light-Matter Interaction, Cooperativities, and Steady-State Entanglement Using Parametric Amplification. *Phys. Rev. Lett.* **120**, 093601 (2018).
68. Glauber, R J. The Quantum Theory of Optical Coherence. *Phys. Rev.* **130**, 2529 (1963).
69. Birnbaum, K M, Boca, A and Miller, R *et al.* Photon blockade in an optical cavity with one trapped atom. *Nature (London)* **436**, 87 (2005).
70. Dayan, B, Parkins, A S and Aoki, T *et al.* A Photon Turnstile Dynamically Regulated by One Atom. *Science* **319**, 1062 (2008).
71. Hamsen, C, Tolazzi, K N and Wilk, T. Strong coupling between photons of two light fields mediated by one atom. *Nat. Phys.* **14**, 885 (2018).
72. Hennessy, K, Badolato, A and Winger, M *et al.* Quantum nature of a strongly coupled single quantum dot–cavity system. *Nature (London)* **445**, 896 (2007).
73. Faraon, A, Fushman, I and Englund, D *et al.* Coherent generation of non-classical light on a chip via photon-induced tunnelling and blockade. *Nat. Phys.* **4**, 859 (2008).
74. Imamoglu, A, Schmidt, H and Woods, G. Strongly Interacting Photons in a Nonlinear Cavity. *Phys. Rev. Lett.* **79**, 1467 (1997).

75. Scully, M O and Zubairy, M S. *Quantum optics* (Cambridge University Press, Cambridge, England, 1997).
76. Agarwal, G S. *Quantum optics* (Cambridge University Press, Cambridge, England, 2012).
77. Johansson, J, Nation, P and Nori, F. QuTiP: An open-source Python framework for the dynamics of open quantum systems. *Comput. Phys. Commun.* **183**, 1760 (2012).
78. Johansson, J, Nation, P and Nori, F. QuTiP 2: A Python framework for the dynamics of open quantum systems. *Comput. Phys. Commun.* **184**, 1234 (2013).
79. Plenio, M B and Knight, P L. The quantum-jump approach to dissipative dynamics in quantum optics. *Rev. Mod. Phys.* **70**, 101 (1998).
80. Wang, Y D and Clerk, A A. Reservoir-Engineered Entanglement in Optomechanical Systems. *Phys. Rev. Lett.* **110**, 253601 (2013).
81. Jiao, Y F, Zhang, S D and Zhang, Y L *et al.* Nonreciprocal Optomechanical Entanglement against Backscattering Losses. *Phys. Rev. Lett.* **125**, 143605 (2020).
82. Liu, J X, Yang, J Y and Lu, T X *et al.* Phase-controlled robust quantum entanglement of remote mechanical oscillators. *Phys. Rev. A* **109**, 023519 (2024).
83. Li, Y, Jiao, Y F and Liu, J X *et al.* Vector optomechanical entanglement. *Nanophotonics* **11**, 67–77 (2022).
84. Hauer, B D, Combes, J and Teufel, J D. Nonlinear Sideband Cooling to a Cat State of Motion. *Phys. Rev. Lett.* **130**, 213604 (2023).

85. Li, B, Qin, W and Jiao, Y F *et al.* Optomechanical Schrödinger cat states in a cavity Bose-Einstein condensate. *Fundam. Res.* **3**, 15–20 (2023).
86. Liao, J Q and Tian, L. Macroscopic Quantum Superposition in Cavity Optomechanics. *Phys. Rev. Lett.* **116**, 163602 (2016).
87. Muñoz, C S, del Valle, E and González Tudela, A *et al.* Emitters of N-photon bundles. *Nat. Photonics* **8**, 550–555 (2014).
88. Bin, Q, Lü, X Y and Laussy, F P *et al.* N-Phonon Bundle Emission via the Stokes Process. *Phys. Rev. Lett.* **124**, 053601 (2020).
89. Bin, Q, Wu, Y and Lü, X Y. Parity-Symmetry-Protected Multiphoton Bundle Emission. *Phys. Rev. Lett.* **127**, 073602 (2021).
90. Zou, F, Li, Y and Liao, J Q. Dynamical N-photon bundle emission. *New J. Phys.* **25**, 043027 (2023).